Transaction on Nano Physics, NEMS & MEMS
ISSN: 2229-8711 Online Publication, June 2011
www.pcoglobal.com/gjto.htm
NP-C10/GJTO

GJTO Global Journal of Technology & Optimization
Volume 2, 2011

A STUDY OF THE CARRIER PROPERTIES OF A GRAPHENE NANORIBBON IN A HIGH MAGNITUDE ELECTRIC FIELD AND ASSOCIATED EFFECTS IN GRAPHENE NANORIBBON TRANSISTORS

N.A. Amin[1], M.T. Ahmadi[1]*, J.F. Webb[2], Z. Johari[1], S. M. Mousavi[1] and R. Ismail[1]

[1]Electronics Engineering Department, Faculty of Electrical Engineering, Universiti Teknologi Malaysia, Skudai, Johor, Malaysia
[2]School of Engineering and Science, Swinburne University of Technology, Sarawak Campus, Kuching, Sarawak, Malaysia
E-mail: *taghi@ieee.org, [2]jeffwebb@physics.org

Received May 2011, Revised May 2011, Accepted June 2011

Abstract
In this paper the high-field behavior of a graphene nanoribbon is studied in the degenerate and non-degenerate regimes. The drift velocity model presented shows that the transport behavior is different in each regime when subject to an electric field. Our theoretical results are compared with experimental data. The Fermi velocity (for the degenerate regime) and thermal velocity (for the non-degenerate regime) coupled with optical phonon emission have a large influence on the drift velocity leading to a velocity saturation preceded by a monotonic increase with increasing electric field. Also the effect of varying the channel length of a transistor employing a graphene channel is considered as well as the influence of the electric field created by the gate voltage.

Keywords: Graphene nanoribbon, transistor, high field carrier transport, drift velocity, mobility.

1. Introduction

A Graphene sheet is a two-dimensional allotrope of sp^2-bonded carbon arranged in a honeycomb lattice [1-3]. A graphene nanoribbon (GNR) however, depicted in Fig. 1, is a strip of graphene with a width of less than 10 nm [4] and shares a number of similarities with a graphene sheet. Much of the interest surrounding graphene is due to the high carrier mobility that it exhibits [1,2,5]. Moreover, carrier velocity control at high electric fields is essential in graphene field effect transistor (GFET), especially for GFET applications in the radio frequency region [6]. This makes graphene a material of great promise as an active element in electronic devices, particularly those based on low-noise, high-frequency operation. The modeling and simulation of high-field (~ 1 V/μm) [7] mobility and velocity saturation effects are important for predicting device characteristics. Furthermore, velocity saturation of carriers in a transistor channel is an important effect that occurs in nano-sized channels and thus it is of interest to gain an understanding of velocity saturation in nanoscale devices.

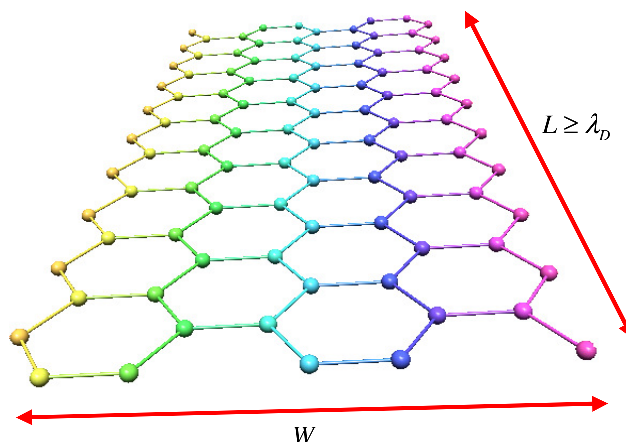

Figure 1: Structure of monolayer GNR: length L, width, W and De Broglie Wavelength, λ_D.

This can be done if quantities such as the density of states (DOS) and low field mobility are obtained.
Here, we use some previous work on low field mobility modeling [8] both in the degenerate and non-degenerate regimes to analyze the drift velocity and hence the high field mobility. Existing work on high field transport [6,9,10] mostly discusses the influence of the optical phonons which limit the velocity as well as the current-carrying capacity under high electric fields. However, our work is not only limited to phonon emission; we also consider high field transport both in the degenerate (high carrier concentration) and non-degenerate (temperature dependent) regimes. Simple analytical models are used to demonstrate the carrier velocity and mobility in both regimes as will be discussed in details in the subsequent subsections.

2. Mobility

Based on a previous model for low field mobility in GNRs by Amin et al. [8], the mobility is deduced from the fundamental transport equation given by:

Copyright @ 2011/gjto

$$\mu = \frac{q\tau}{m^*} = \frac{q\ell_0}{m^* v} \quad (1)$$

Applying the above expression to parabolic band energy and making use of the Fermi-Dirac integral, we obtain the low field mobility for the degenerate and non-degenerate regimes, which depends on the carrier concentration and temperature respectively. The low-field mobility equations for the degenerate, μ_{0D_GNR} and non-degenerate regimes, μ_{0ND_GNR} are:

$$\mu_{0ND_GNR} = v_{th} \frac{q\ell_0}{m^* v_{th}\sqrt{\pi}} \quad (2)$$

where v_{th} is the thermal velocity, and

$$\mu_{0D_GNR} = \frac{q\ell_0 \hbar\left(\sqrt{\pi} n_1\right)}{4m^* k_B T\sqrt{2}} \quad (3)$$

with the carrier concentration in a one-dimensional device denoted by n_1. At low appied electric field magnitudes, the carrier mobility does not depend on the electric field and the velocity saturation does not take place at all. However, as the electric field comes into play, the transport behavior will differ from the one observed for low fields as the quantum emission will influence the transport in a high field. This is because the electrons are accelerated by the field and hence gain enough energy to emit phonons. The photon energy is $\hbar\omega$ where ω is the angular frequency of the associated wave [11]

3. Drift velocity

The drift velocity, v_d in a high electric field, E is given by [7, 12]:

$$v_d(E) = \frac{\mu_0 E}{1 + \mu_0 E / v_{sat}} \quad (4)$$

where μ_0 is the low field mobility and v_{sat} is the saturation velocity, which refers to the thermal and Fermi velocity for non-degenerate and degenerate regimes respectively, as suggested by Saad et al. [13]. In the work here, we apply the low field mobility model [8] to Eq. (4) for both the degenerate and non-degenerate regimes. The drift velocity in Eq. (4) is also known as it depends on the horizontal electric field. This horizontal electric field exists due to the source-drain voltage, and thus is given by the voltage drop across the channel over the channel length, L_{CH} [14]:

$$E = \frac{V_{DS}}{L_{CH}} \quad (5)$$

The effects of varying the channel length can be observed by incorporating Eq. (5) into Eq. (4). Below are the calculated results for drift velocity effects in the degenerate regime found for channel lengths 32nm, 22nm and 16nm?

In both the degenerate and non-degenerate cases, a shorter channel length produces a higher drift velocity due to the longer mean free path (mfp) of the carriers compared to the channel length. The carrier mfp is 0.4 μm in the degenerate regime and 1.2 μm in the non-degenerate regime compared to the channel length of 16nm.

However, a vertical electric field also exists, due to the applied gate voltage V_{GS} which also influences the carrier velocity. This vertical electric field forces the carriers to move closer to the

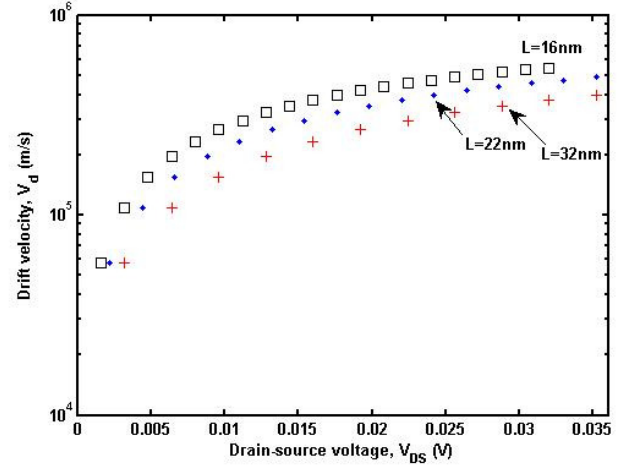

Figure 2: Channel length effects on the drift velocity in the degenerate regime.

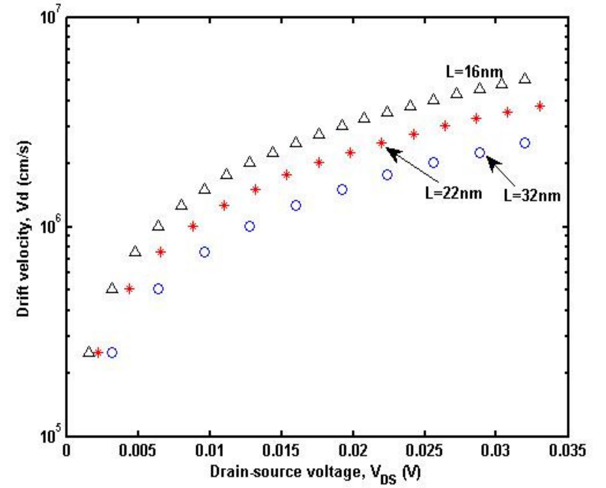

Figure 3: Channel length effects on the drift velocity in the non-degenerate regime.

channel surface in which the carrier movement from source to drain will be reduced because surface scattering is dominant at the channel interface and hence the mobility is reduced. The carrier mobility can then be represented by an effective mobility given by [14]:

$$\mu_{eff} = \frac{\mu_0}{1 + \theta\left(V_{GS} - V_T\right)} \quad (6)$$

3. 1. Drift velocity in the degenerate regime

Interestingly, it is found from our calculations that the drift velocity in the degenerate regime is slightly higher than the experimental result, as depicted in Fig.4. the calculated drift velocity is comparable with the experimental drift velocity for horizontal electric field values below 0.5 V/μm and tends to reach a saturation velocity more slowly compared to the experimental saturation velocity. Besides this, the higher drift velocity indicates that the mobility is also high. The mobility can be found by measuring the gradient of the drift velocity versus electric field graph.

3. 2. Drift velocity in the non-degenerate regime

In the non-degenerate regime, the difference between the calculated and experimental results is the other way around: the experimental drift velocity is higher, as shown in Fig. 5.

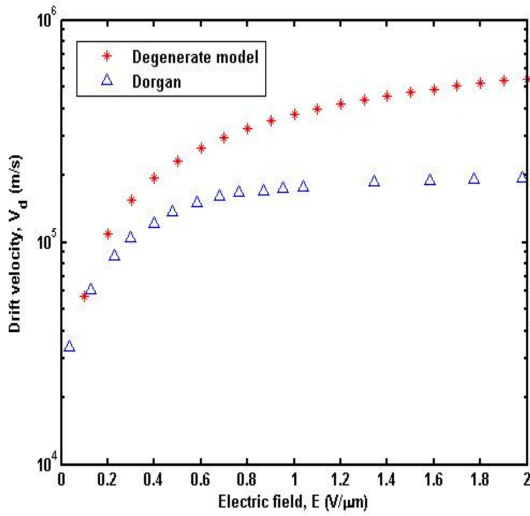

Figure 4: Comparison of the high field degenerate model with the experimental data of Dorgan et al. [7].

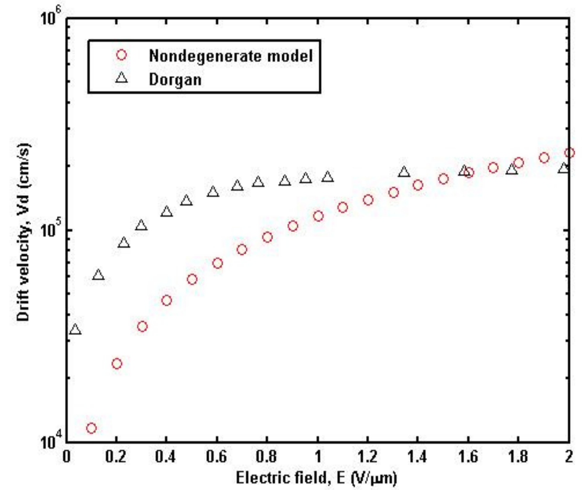

Figure 5: The non-degenerate model compared with the experimental data of Dorgan et al. [7].

In this region, the calculated drift velocity is lower than the experimental drift velocity but reaches the same saturation level for a high electric field of 2 V/μm . This is because the thermal velocity plays an important role in determining the drift velocity in the presence of an applied electric field. Carriers travel with a thermal velocity in the non-degenerate regime where the carrier density is lower. The thermal velocity is $v_{th} = \sqrt{2k_B T} \approx 8\times10^5$ m/s for the one-dimensional case [10]. This is adequate since we consider a GNR as a one-dimensional device. Returning to the drift velocity: the lower drift velocity also the mobility is low compared to the experimental results and compared to the degenerate mobility.

Optical phonon emission in graphene is dominant in the presence of a high electric field with carrier energies in the range 10 meV to 200 meV [7,10]. This is enough for optical phonons to be emitted and we expect this strong enhancement of optical phonon emission to prevent the carriers in the GNR from gaining larger velocities with further increases in electric field. In other words, the optical phonon emission is the main cause of the scattering that limits the drift velocity such that it reaches saturation. This also holds true in the high electric field experimental and theoretical studies in Refs. [11,15]. Additionally, Tse et al. [10] have found that in doped graphene (high carrier concentration), the scattering process termed 'hot electron scattering', for energies below 200 meV, is dominated by inelastic scattering, whereas for carriers having energies above 200 meV, the scattering due to the electron-phonon interactions tends to dominate as the carriers are now able to emit longitudinal optical phonons. These hot carriers are responsible for reducing the mobility at high electric field magnitudes. The observation that the drift velocity in the degenerate regime is higher than that for the non-degenerate regime (see Fig. 6) can be explained as being due to the different velocities of the carriers in each regime: in the degenerate regime the velocity is the Fermi velocity of graphene, $v_f \approx 9.8\times10^5$ m/s [16], which is higher than the thermal velocity and gives an extra advantage to the carriers in the degenerate regime.

4. Conclusion

The drift velocity in the degenerate regime ($\approx 5.4\times10^5$ m/s), is higher than the drift velocity in the non-degenerate regime

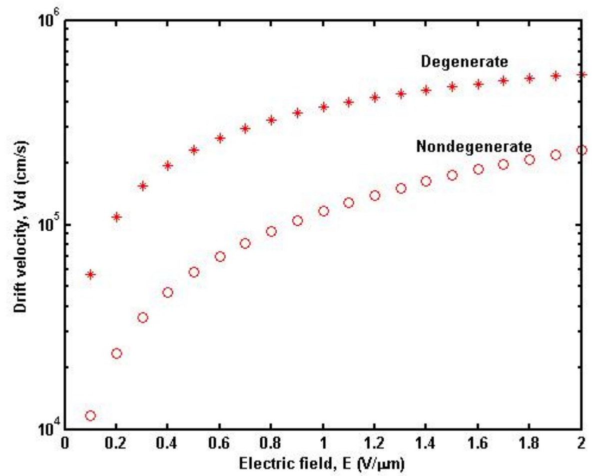

Figure 6: Comparing the degenerate and non-degenerate drift velocity models.

($\approx 1.8\times10^5$ m/s) leading to better performance for devices operating in the degenerate regime. This is because the carriers in the degenerate regime travel with the Fermi velocity which is higher than the thermal velocity in the non-degenerate regime. The Fermi velocity (degenerate regime) and thermal velocity (non-degenerate regime) coupled with optical phonon emission greatly influenced the drift velocity in the respective cases leading to velocity saturation. Consequently, the carrier mobility also tends to be constant as the drift velocity no longer increases. Besides this, a shorter channel length, which is essential in order to reduce the device dimensions, offers a higher carrier drift velocity. This is consistent with our calculated results, and is due to the longer mfp of carriers in GNRs compared to the transistor's channel length.

This work has elucidated the degenerate and non-degenerate carrier transport behavior in GNRs. Further investigation is needed to confirm this theoretical study especially for the high electric fields in which many technologically important electronic devices operate.

Acknowledgments

The authors from the Universiti Teknologi Malaysia (UTM) would like to thank the Ministry of Science, Technology and Innovation (MOSTI), Malaysia, together with the Research Management Center at UTM for generous financial support.

Copyright @ 2011/gjto

References

[1] K. Novoselov, A. K. Geim, S. Morozov, D. Jiang, Y. Zhang, S. Dubonos, I. Grigorieva, and A. Firsov, "Electric Field Effect in AtomicallyThin Carbon Films," Science, vol. 306, 2004,
pp. 666-669.

[2] A. K. Geim and K. Novoselov, "The Rise of Graphene," *Nature Materials*, vol. 6(3), 2007, pp. 183-191.

[3] S. M. M. Dubois, Z. Zanolli, X. Declerck, and J. C. Charlier, "Electronic Properties and Quantum Transport in Graphene-based Nanostructures," *European Physical Journal B*, 72(1) 2007, pp. 1-24.

[4] L. Jiao, L. Zhang, X. Wang, G. Diankov, and H. Dai, "Narrow Graphene Nanoribbon from Carbon Nanotubes," *Nature*, vol. 458(7240), 2009, pp. 877-880.

[5] K. I. Bolotin, K. J. Sikes, Z. Jaing, M. Klima, G. Fudenberg, J. Hone, P. Kim, and H. L. Stormer, "Ultrahigh Electron Mobility in Suspended Graphene," *Solid State Commun.*, vol. 146, 2008, pp. 351-355.

[6] A. M. DaSilva, K. Zou, J. K. Jain, and J. Zhu, "Mechanism for Current Saturation and Energy Dissipation in Graphene Transistors," *Physical Review Letters*, vol. 104, 2010, p. 236601,

[7] V. E. Dorg, M. H. Ba, and E. Po, "Mobility and Saturation Velocity in Graphene on SiO_2" *Applied Physics Letters* 97(8), 2010, pp.082112-082113.

[8] N. A. Amin, Z. Johari, M. T. Ahmadi, and R. Ismail, "Low-field Mobility Model on Parabolic Band Energy of Graphene Nanoribbon," *Modern Physics Letters B* 25(4), 2010, pp.281-290.

[9] D. Jena, "A Theory for The High-field Current Carrying Capacity of One-dimensional Semiconductors," *Journal of Applied Physics*, vol.105, 2009, p. 123701.

[10] W. K. Tse, E. H. Hwang, and S. D. Sarma, "Ballistic Hot Electron Transport in Graphene," *Applied Physics Letters*, vol. 93, 2008, p. 023128.

[11] Z. Yao, C. Kane, and C. Dekker, "High-field Electrical Transport in Single-wall Carbon Nanotubes," *Physical Review Letters*, vol. 84, 2000, p. 2941.

[12] B. W. Scott and J. P. Leburton, "High Field Carrier Velocity and Current Saturation in Graphene Field-effect Transistors," 10th IEEE Conference on. Nanotechnology (IEEE-NANO), 2010, pp.655-658.

[13] I. Saad, M. L. P. Tan, I. H. Hii, R. Ismail, and V. K. Arora, "Ballistic Mobility and Saturation Velocity in Low-dimensional Nanostructures," *Microelectronics Journal*, vol. 40(3), 2009, pp. 540-542.

[14] Paul R. Gray, Paul J. Hurst, Stephen H. Lewis and Robert G. Meyer, Analysis and Design of Analog Integrated Circuits (5th Ed.), John Wiley & Sons, New Jersey, 2010.

[15] V. K. Arora, "Quantum engineering of nanoelectronic devices: the role of quantum emission in limiting drift velocity and diffusion coefficient," *Microelectronics Journal*, vol. 31(11-12), 2000, pp.853-859.

[16] O. V. Kibis, M. R. da Costa, and M. E. Pornoi, "Generation of Terahertz Radiation by Hot Electrons in Carbon Nanotubes," *Nano Letters*, vol. 7(11), 2007, pp. 3414-3417.